Looking Chloride Channels Straight in the Eye: Bestrophins, Lipofuscinosis, and Retinal Degeneration

Criss Hartzell, Zhiqiang Qu,
Ilva Putzier, Liana Artinian,
Li-Ting Chien,
and Yuanyuan Cui

Department of Cell Biology,
The Center for Neurodegenerative Disease,
Emory University School of Medicine,
Atlanta, Georgia
criss.hartzell@emory.edu

Recent evidence suggests that Cl⁻ ion channels are important for retinal integrity. Bestrophin Cl⁻ channel mutations in humans are genetically linked to a juvenile form of macular degeneration, and disruption of some ClC Cl⁻ channels in mice leads to retinal degeneration. In both cases, accumulation of lipofuscin pigment is a key feature of the cellular degeneration. Because Cl⁻ channels regulate the ionic environment inside organelles in the endosomal-lysosomal pathway, retinal degeneration may result from defects in lysosomal trafficking or function.

Your ability to read this article without magnification requires the normal functioning of your macula. The macula is a small region near the center of the retina responsible for high-acuity vision due to its high density of cone photoreceptors. Almost everyone knows somebody, often a parent or grandparent, who has the progressive disorder known as macular degeneration. When it occurs beyond the 5th decade of life and has no specific diagnosis, it is called "age-related macular degeneration" (AMD). AMD is the leading cause of blindness in technologically developed countries (57). (World wide, cataracts, trachoma, and glaucoma rank higher.) AMD has been estimated to affect ~20% of the population over the age of 65 and >35% of individuals over the age of 75 (73).

Macular Degeneration is Often Associated with Retinal Lipofuscinosis

Macular degeneration is a heterogeneous collection of diseases with multiple causes. Genes linked to macular degeneration encode proteins of diverse function: these include enzymes that remodel extracellular matrix, an ATP-binding cassette transporter, and immune complement factor H (17, 30, 31, 53). A common feature of several types of macular degeneration is the accumulation of lipofuscin pigment in and around the retinal pigment epithelium (RPE) (FIGURE 1). Lipofuscin is a heterogeneous mixture of both proteins and lipids that are partially oxidized (67). It is thought that lipofuscin accumulation is a major causal factor in AMD because it correlates with the severity of photoreceptor degeneration (94) and has been shown to have toxic properties (21, 68). The major fluorescent component of lipofuscin is *N*-retinylidene-*N*-retinylethanolamine (A2E), which is a metabolite of retinal, visual pigment. A2E has been shown to perturb lysosomal function (21, 68), disrupt membrane integrity by a detergent-like effect (19), and promote programmed cell death (70). Proteomic analysis shows that various components of lipofuscin are derived both from photoreceptors and RPE (67). A possible explanation of this dual cellular origin is provided by the fact that photoreceptor outer segments are renewed by the daily phagocytosis of the tips of photoreceptors by RPE cells (5, 54). It would therefore make sense if lipofuscin accumulation were related to a problem of phagocytosis or lysophagosome function (18).

In any case, lipofuscin seems to be a noxious material. Lipofuscin accumulation is also associated with a group of neurodegenerative diseases called neuronal ceroid lipofuscinoses (NCLs). NCLs are lysosomal storage diseases characterized by accumulation of lipofuscin pigment, blindness due to retinal degeneration, psychomotor retardation, and premature death (15, 27, 52). Because some genes associated with NCLs code for proteins critical for lysosomal function (12), this raises the possibility that lysosomal dysfunction may also be involved in AMD.

Best Disease May Be a Model for Macular Degeneration

Both genetic and environmental factors contribute to AMD, but there are a number of early-onset forms of macular degeneration that are exclusively or largely genetic. One of these diseases is Best vitelliform macular dystrophy (also called Best disease), which is inherited in an autosomal-dominant manner and is linked to mutations in the bestrophin-1 gene located on chromosome 11 (11q13). In Best disease, lipofuscin accumulates within macrophages in the subretinal space, in RPE cells, and between RPE cells and photoreceptors. The gene responsible for Best disease was positionally cloned in 1998 from families exhibiting macular degeneration with a juvenile age of onset (48, 58). Over 85 human bestrophin-1 (hBest1) mutations are now associated with macular degeneration (FIGURE 2) (see Ref. 88 and the Human Gene Mutation Database at http://uwcmml1s.uwcm.ac.uk/uwcm/mg/search/133795.html). In addition, inherited abnormal splice variants of hBest1 are associated with autosomal-dominant vitreoretino choroidopathy, a retinal dystrophy that is associated with defects of ocular

development such as nanophthalmos (92).

Best Disease May Be a Chloride Channelopathy

Although it was initially hypothesized that hBest1 might be a transporter of lipid components of lipofuscin (58), there is now considerable evidence that bestrophins function as Cl⁻ channels. After hBest1 was cloned, Jeremy Nathans' lab expressed hBest1 in human embryonic kidney 293 cells and showed that its expression was associated with appearance of a novel Ca^{2+}-sensitive Cl⁻ current (74). Our lab and Nathans' lab have now shown that bestrophins from human, mouse, *Xenopus*, *Caenorhabditis elegans*, and *Drosophila* function as Cl⁻ channels when expressed heterologously (62, 74, 79). Subsequently, work from our lab showed that the Ca^{2+} sensitivity was in the physiological range, with an EC_{50} for Ca^{2+} of ~200 nM (62). The Ca^{2+} sensitivity of hBest1, mouse (m)Best2, and *Xenopus* Best2 are similar, but the Ca^{2+} sensitivity of other bestrophins has not yet been published. Whether bestrophins are regulated by direct Ca^{2+} binding, by calmodulin, or by Ca^{2+}-dependent phosphorylation (32) is not known.

Role of Cl⁻ channels in Best disease

The suggestion that bestrophins are Cl⁻ channels is particularly intriguing because the hallmark diagnostic feature of Best disease is a decreased slow light peak in the electrooculogram (EOG) (FIGURE 3). The slow light peak is thought to reflect a Cl⁻ conductance in the basolateral membrane of the RPE (24). Because Best1 is localized at the basolateral membrane of the RPE (4, 46), the idea that Best1 is responsible for the basolateral Cl⁻ conductance is particularly attractive.

The mechanisms linking Cl⁻ channel dysfunction to the macular dystrophy that ensues is not clear. This is partly because visual acuity in Best disease patients is highly variable. For example, in one family, an elderly mother
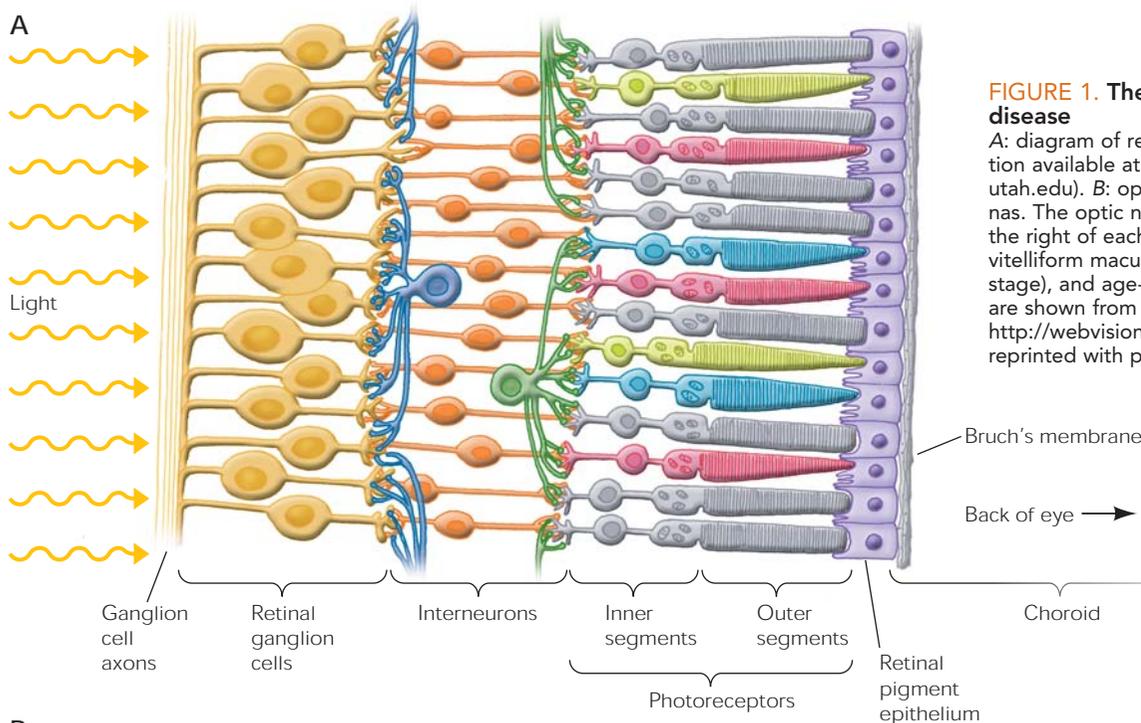

FIGURE 1. **The retina in health and disease**
A: diagram of retina (redrawn from an illustration available at http://webvision.med.utah.edu). *B*: ophthalmoscopic images of retinas. The optic nerve is the yellowish spot on the right of each retina. Normal retina, Best vitelliform macular dystrophy (vitelliform stage), and age-related macular degeneration are shown from *left* to *right*. (Images are from http://webvision.med.utah.edu/ and are reprinted with permission).
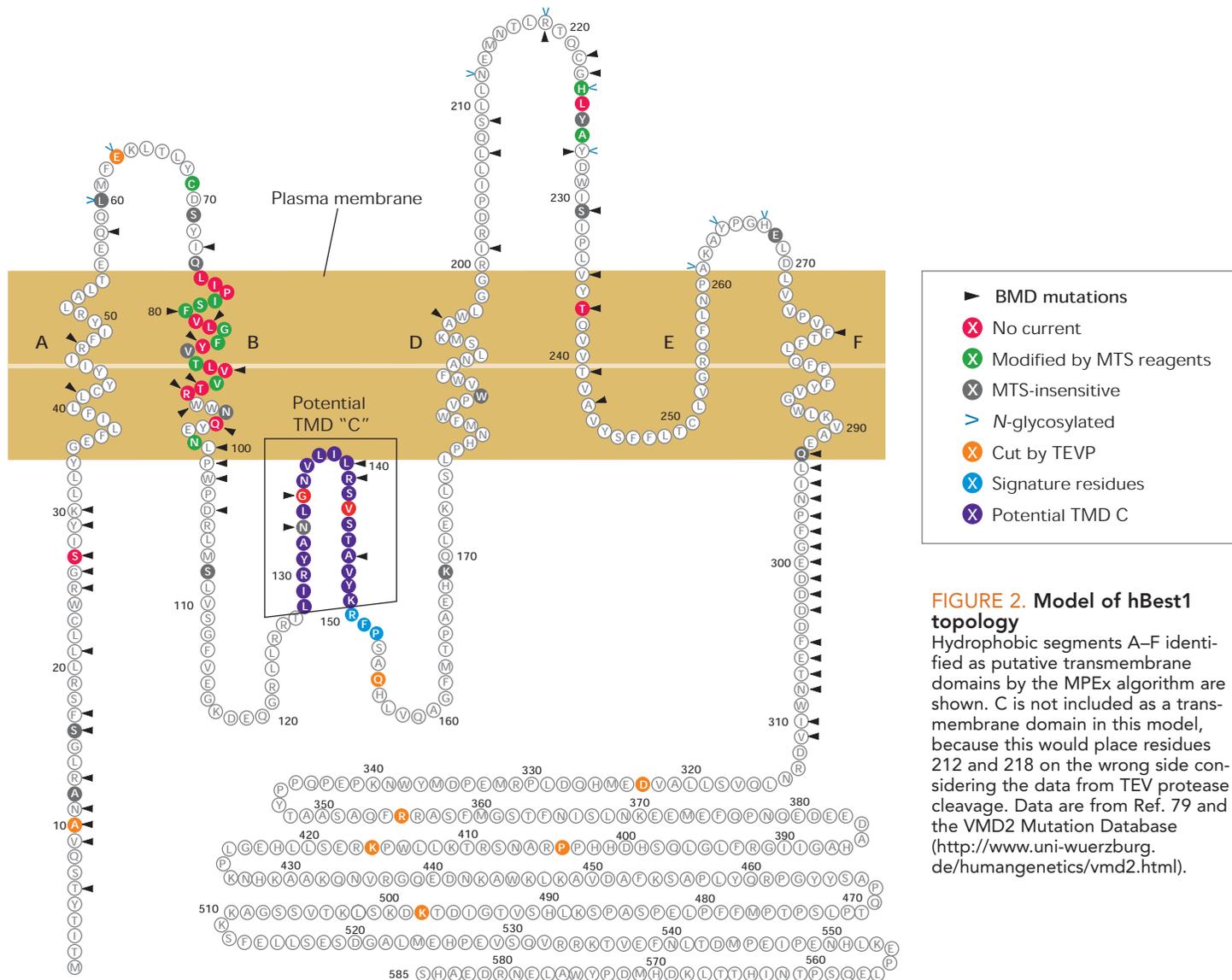
FIGURE 2. Model of hBest1 topology
Hydrophobic segments A–F identified as putative transmembrane domains by the MPEx algorithm are shown. C is not included as a transmembrane domain in this model, because this would place residues 212 and 218 on the wrong side considering the data from TEV protease cleavage. Data are from Ref. 79 and the VMD2 Mutation Database (http://www.uni-wuerzburg.de/humangenetics/vmd2.html).

had normal visual acuity of 20/20, whereas her daughter and three grandchildren had clinical symptoms as early as age 5, even though all had the same genotype (R218C/+) (10). Despite the variable penetrance of disease symptoms, virtually all individuals with bestrophin gene mutations exhibit abnormal EOGs (81). This suggests that other factors, genetic or environmental, must contribute to the development of retinal lesions. However, the fact that an abnormal EOG is a consistent feature of the disease but that degraded visual acuity is more variable provides a strong argument that Cl⁻ channel dysfunction precedes macular degeneration.

Because an abnormal EOG is unambiguously linked to hBest1 mutations, it would be useful to understand the mechanism of the light peak, but this also remains somewhat obscure. To measure the EOG, electrodes are placed on either side of the eye, then the subject is allowed to adapt to darkness and is asked to fixate on one of two light-emitting diodes 30° apart that illuminate alternately at a frequency of ~0.2/s. The difference in voltage measured when the eyes are fixated on the right vs. the left light-emitting diode is thought to represent the voltage across the RPE. During dark adaptation, the potential becomes small (the dark trough) (FIGURE 3). When the ambient lights are turned on, the potential increases slowly to reach a peak in ~5–15 min (light peak). The EOG obviously is an indirect measure of changes in conductance that occur in the retina. The electroretinogram (ERG), which measures the potential across the retina directly, might provide a more direct measurement of the electrical changes. However, there are technical obstacles to using direct-current ERG (dcERG) to record the very-long-duration light peak in humans. Conventional full-field ERGs, which are taken on a much shorter time scale, are often reported to be normal in Best disease. Multifocal ERGs, which use multiple electrodes to sort out spatial differences in retinal function, usually reveal central amplitude

reductions in patients with clinical symptoms (65). These ERG abnormalities are probably not related to the slow light peak of the EOG but probably reflect degenerative changes secondary to the initial vitelliform lesions.

In animals, dcERG recordings show a slow light peak that has the same time course as the slow light peak in the EOG, suggesting that the slow light peaks in the dcERG and EOG have the same cellular basis. The slow light peak in the dcERG clearly originates from changes in a basolateral conductance in the RPE cells (41). The 5- to 15-min time course of the slow light peak suggests that its mechanisms could be quite complex. It has been proposed that a diffusible substance is released from the neural retina that activates the Cl$^-$ conductance in the RPE (41), but the identity of the light substance remains unknown (see discussion in Refs. 24 and 91).

Support for the idea that bestrophin is a basolateral Cl$^-$ channel in RPE is provided by recent experiments from Marmorstein's lab (47). In these experiments, an adenovirus encoding either wild-type human Best1 or disease-causing W93C or R218C mutants of hBest1 were injected into the eyes of young rats. The corresponding proteins were found to be expressed in the basolateral membrane of the RPE by immunostaining. Expression of the W93C mutants decreased the light peak of the dcERG without affecting other components of the dcERG. This is the expected result if W93C bestrophin is dominant negative in inhibiting the function of the endogenous wild-type bestrophin. Best disease caused by the W93C mutation is inherited in a dominant fashion, and the W93C mutant has been shown to inhibit wild-type currents in expression systems (62, 74). The effects of the R218C mutant were less than those of the W93C mutant, but the R218C mutation may produce less-severe disease as well. Despite these positive results, the authors express reservations about concluding that bestrophin is the basolateral Cl$^-$ conductance, because the effects of over-
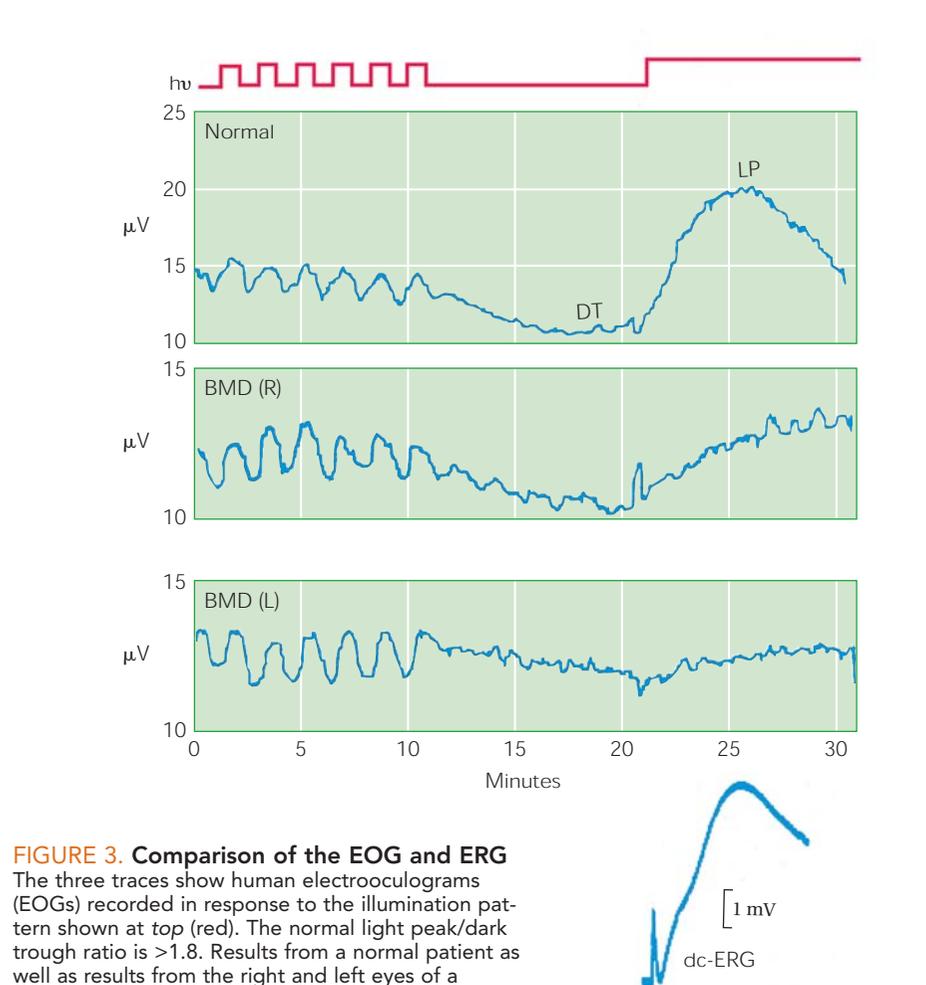

FIGURE 3. Comparison of the EOG and ERG
The three traces show human electrooculograms (EOGs) recorded in response to the illumination pattern shown at *top* (red). The normal light peak/dark trough ratio is >1.8. Results from a normal patient as well as results from the right and left eyes of a patient with Best disease [BMD (R) and BMD (L), respectively] are shown; this BMD patient had normal visual acuity of 20/16. Data are from Ref. 85. The trace at *bottom* shows a direct-current electroretinogram (dcERG) from a cat on the same time scale as the EOG records at *left*. The sharp spike corresponds to the c-wave of the ERG and is followed by the light peak, which has the same time course as the LP of the EOG. Data are from Ref. 41.

expression of the W93C mutant on the light peak are considerably less than they expected considering the amount of overexpression. Furthermore, overexpression of wild-type hBest1 did not increase the light peak as expected. However, this might simply mean that the endogenous channels alone produced a maximal response.

What is the evidence that hBest1 is a Cl$^-$ channel?

As mentioned above, expression of several bestrophins in 293 cells induces a novel Ca^{2+}-activated Cl$^-$ current. Unfortunately, identification of Cl$^-$ channels by heterologous expression has a troubled history (11, 35). There are a number of proteins, including p64, the CLICs, and

the CLCAs, whose Cl$^-$ channel function is doubted even though they induce Cl$^-$ currents when overexpressed. For the CLICs and p64, skepticism derives from the fact that their structure (small size and only one or no predicted transmembrane domain) seems incompatible with an ion channel. With the CLCAs, there also is disagreement as to whether they are integral membrane proteins (26). A more general problem is that many Cl$^-$ currents are biophysically similar and very few specific blockers have been identified. Consequently, it is often difficult to be certain that an expressed protein is not simply upregulating an endogenous Cl$^-$ channel: every cell has endogenous Cl$^-$ channels and these channels may not be easily separated from the

heterologously overexpressed currents.

With bestrophins, considerable evidence has accumulated to establish that these proteins can function as Cl⁻ channels, although there is the possibility they have other functions as well. Several different arguments support the idea that bestrophins are Cl⁻ channels.

1) Bestrophins from different species expressed in 293 cells produce novel Ca^{2+}-activated Cl⁻ currents (62, 74). The type of current that is induced is the same in different cell lines (61). Because one would not necessarily expect upregulation of the same kind of Cl⁻ channel in different cell types, the appearance of similar currents in different cells minimizes (but does not eliminate) the concern over upregulation of endogenous channels (61).

2) In mammals, there are four bestrophin genes (40, 79). In *C. elegans*, there are at least 25 different bestrophins. Different bestrophins produce currents with different characteristics (74, 79). For example, hBest1 currents have linear current-voltage relationships and are essentially time independent, whereas hBest3 currents strongly inwardly rectify and activate slowly with time (79). These different characteristics provide some confidence that the currents are specific to the type of bestrophin expressed.

3) hBest1 and mBest2 currents are inhibited by the modification of sulfhydryl groups with membrane-impermeant MTSET⁺ (61, 63, 79). Modification of ionic currents by MTSET⁺ is a common approach used to identify amino acids that line the permeation pathway (36).

4) Expression of dominant-negative mutants of bestrophin, notably G299E and W93C, inhibit the current induced by expression of the wild-type bestrophin (62, 74), suggesting that the channels are multimers. Semiquantitative co-immunoprecipitation shows that

bestrophins form multimeric complexes composed of four or five subunits, as one would expect for a channel protein (74).

5) Point mutations in both hBest1 and mBest2 produce changes in Cl⁻ channel function. Most notably, certain mutations change the selectivity of the channel for anions and/or change channel gating, as described below. Because it is generally agreed that the selectivity of a channel is determined by the channel pore, the ability to change the selectivity by a mutation provides strong evidence that bestrophin is responsible for forming the channel (60).

The Transmembrane Topology of Bestrophin Remains in Question

In discussing the structure-function of bestrophins, it is useful first to consider their transmembrane topology (FIGURE 2). Several different models of bestrophin topology have been proposed based on conventional hydropathy analysis, but the only model to have serious experimental support is the one proposed by Nathans' lab (79). Nathans' model for hBest1 proposes four transmembrane domains and a loop. This model is supported by experiments examining the glycosylation of inserted *N*-glycosylation sites and cleavage of inserted tobacco etch virus (TEV) protease sites. They also inferred the topology by substituting various amino acids with cysteine and testing the effects of the membrane-impermeant sulfhydryl reagent MTSET⁺ on the currents (79). Modification of the currents by extracellular MTSET shows that the residue is accessible to the extracellular solution. Although their model is a useful starting point, we feel that the model remains incomplete, because no direct data exists for the sidedness of residues 100–211, but transmembrane prediction by several algorithms, including MPEx (89), suggests that there is a transmembrane domain in this region (FIGURE 2). In their model (79), the segment centered on

138 is not considered to be transmembrane.

Mutagenesis of the second transmembrane domain

We have studied mBest2 as a model for bestrophin Cl⁻ channel function and have mutated a number of residues that either alter the selectivity of the channel for anions or alter channel gating. We have focused on the putative second transmembrane domain (TMD2) partly because this region is one of the most conserved regions in the bestrophins and is the location of a number of disease-causing mutations in hBest1. Also, the finding in hBest1 that residues C69 and N99 are at opposite ends of the predicted transmembrane segment but are both accessible to MTSET applied extracellularly (79) is consistent with TMD2 forming the pore.

Replacing any of several native amino acids in mBest2 TMD2 with cysteine alters the relative permeability of the channel for anions (61, 63). For example, the S79C mutation has a lower relative permeability to SCN⁻ (P_{SCN}/P_{Cl}) than wild-type channels, but the relative SCN⁻ conductance (G_{SCN}/G_{Cl}) is increased. This suggests that the affinity of a binding site in the channel pore is reduced for SCN⁻ relative to Cl⁻ (61). This suggestion is confirmed by measuring the ability of SCN⁻ to compete for Cl⁻ moving through the channel. In wild-type mBest2, SCN⁻ inhibits Cl⁻ currents with an EC_{50} of 12 mM, whereas in the S79C mutant the EC_{50} for SCN⁻ is immeasurably large. These data show clearly that bestrophin can function as a Cl⁻ channel, because the binding site for permeant anions is certainly located in the channel pore (60). Substitution of 15 amino acids with cysteine in TMD2 has similar effects to those just described for S79C, but several substitutions in residues in TMD1 (R34), TMD3 (F149, R150), TMD4 (K180, R196, R197, R200), and the loop (D228, W229, I230) produced wild-type currents (Qu and Hartzell, unpublished observations).

Additional evidence that amino acids 72–95 line the pore is provided

by the effect of charged MTS sulfhydryl reagents on cysteine-substituted mBest2 currents. The effects of the positively charged MTSET⁺ and negatively charged MTSES⁻ on mBest2 currents depend systematically on which residue is changed to cysteine. A helical wheel representation of TMD2 reveals that residues that are insensitive to MTS reagents are clustered on one side of the helix, whereas modifiable residues are concentrated on the other side (FIGURE 4). The fact that changing the electrostatic charge along one side of the TMD2 helix produces changes in Cl⁻ conductance provides important evidence that this part of the protein is involved in forming the pore.

Single-channel recordings of bestrophin currents have not yet been published. Unfortunately, this places some limitations on the conclusions that can be made from the mutagenesis experiments. Whole cell conductance is the product of the number of active channels (N), their mean open probability (p_o), and the single-channel conductance (γ). Although we assume that the effects of MTS reagents reflect changes in γ, another possibility is that these reagents affect channel gating (p_o). Although we cannot eliminate the possibility that TMD2 is involved in channel gating, the effects of cysteine substitution on anion permeability are more simply explained in terms of channel permeability. Nevertheless, mutations in this domain clearly do alter channel gating, as evidenced by the finding that in the S79T mutation G_{SCN}/G_{Cl} changes with time after switching to SCN⁻ (63). Furthermore, we have identified several mutations in TMD2 that dramatically alter channel kinetics (Y. Qu and H. C. Hartzell, unpublished observations).

Location of mutations in hBest1

As mentioned above, in mammals there are generally four bestrophin genes (40, 72). In mouse, one of these appears to be a pseudogene (40). The first ~350 amino acids are highly conserved among subtypes and species, whereas the COOH terminus is quite divergent. For example, hBest1 and mBest1 are 83% identical in the first 350 amino acids but only 44% identical in residues from 350 to the end. The high proline content of the COOH terminus (9%) suggests that this region may be important in protein-protein interactions, but specific motif searches have been disappointing.

The mutations in hBest1 that produce Best disease are scattered throughout the first 312 amino acids but are conspicuously absent after amino acid 312 (FIGURE 2). The mutations are concentrated in the NH₂ terminus, TMD2, hydrophobic segment "C" (residues 130–150), the second extracellular loop and the first part of segment "E," and the ~20 amino acids after the last transmembrane domain. This last region (amino acids 293–311) is highly conserved in all of the bestrophins and is characterized by a cluster of acidic residues. Mutations in 16 of 18 amino acids in this region have been reported to be linked to Best disease. The function of this domain remains unexplored, partly because mutagenesis often pro-
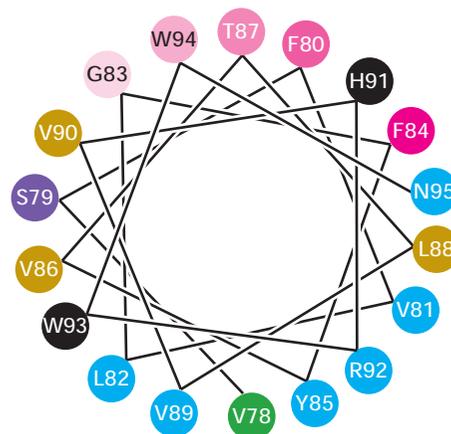

FIGURE 4. Helical wheel representation of amino acids 78–95 of TMD2 of mBest2
Residues were mutated to cysteine, and the effects of MTSET⁺ and MTSES⁻ were examined. Purple: both MTSET⁺ and MTSES⁻ stimulate. Pink to red: MTSET+ stimulates and MTSES⁻ inhibits (the saturation of the color indicates the magnitude of the effect). Blue: neither MTSET⁺ or MTSES⁻ have an effect. Yellow: MTSET⁺ stimulates but MTSES⁻ has no effect. Green: MTSET⁺ inhibits and MTSES⁻ stimulates. Black: no current. Data from Z. Qu, Y. Cui, L.T. Chien, and H.C. Hartzell (unpublished observations).

duces nonfunctional channels (Qu and Hartzell, unpublished observations). Its acidic nature suggests that it could be a site of Ca²⁺ binding, but acidic domains are also a common feature of protein-sorting signals (e.g., see Ref. 43).

Cl⁻ Channels May Play Multiple Roles in Retinal Function

What are the mechanisms that might explain how defects in bestrophin Cl⁻ channel function produce macular degeneration? These mechanisms are summarized in FIGURE 5 and discussed below.

Regulation of the fluid surrounding photoreceptors

RPE cells participate in regulating the volume and ionic composition of the space surrounding photoreceptor outer segments. Epithelial transport across the RPE is mediated by apical (photoreceptor-facing) Na-K-2Cl cotransporters that use the energy from the Na⁺ gradient to move Cl⁻ uphill into the cell and basolateral Cl⁻ channels that allow Cl⁻ ions to flow down their electrochemical gradient toward the choroid (6, 23, 64, 66). RPE polarity is opposite to that found in secretory epithelia, such as parotid gland, where the Na-K-2Cl cotransporter and the Na-K-ATPase are located basolaterally and Cl⁻ secretion occurs via Cl⁻ channels in the apical membrane. Transepithelial movement of Cl⁻ is followed by Na⁺ as counterion to neutralize charge and water to balance osmotic pressure. Thus there is a net flow of NaCl and water from the neural retina to the choroid (77). Light-dependent changes in photoreceptor ionic currents result in significant accumulation and depletion of ions in the space around the photoreceptor outer segments (34), and it is thought that fluid and ion transport by the RPE helps maintain the composition of this fluid within a range that supports phototransduction. Dysfunction of these transport processes would be expected to have pathological consequences.
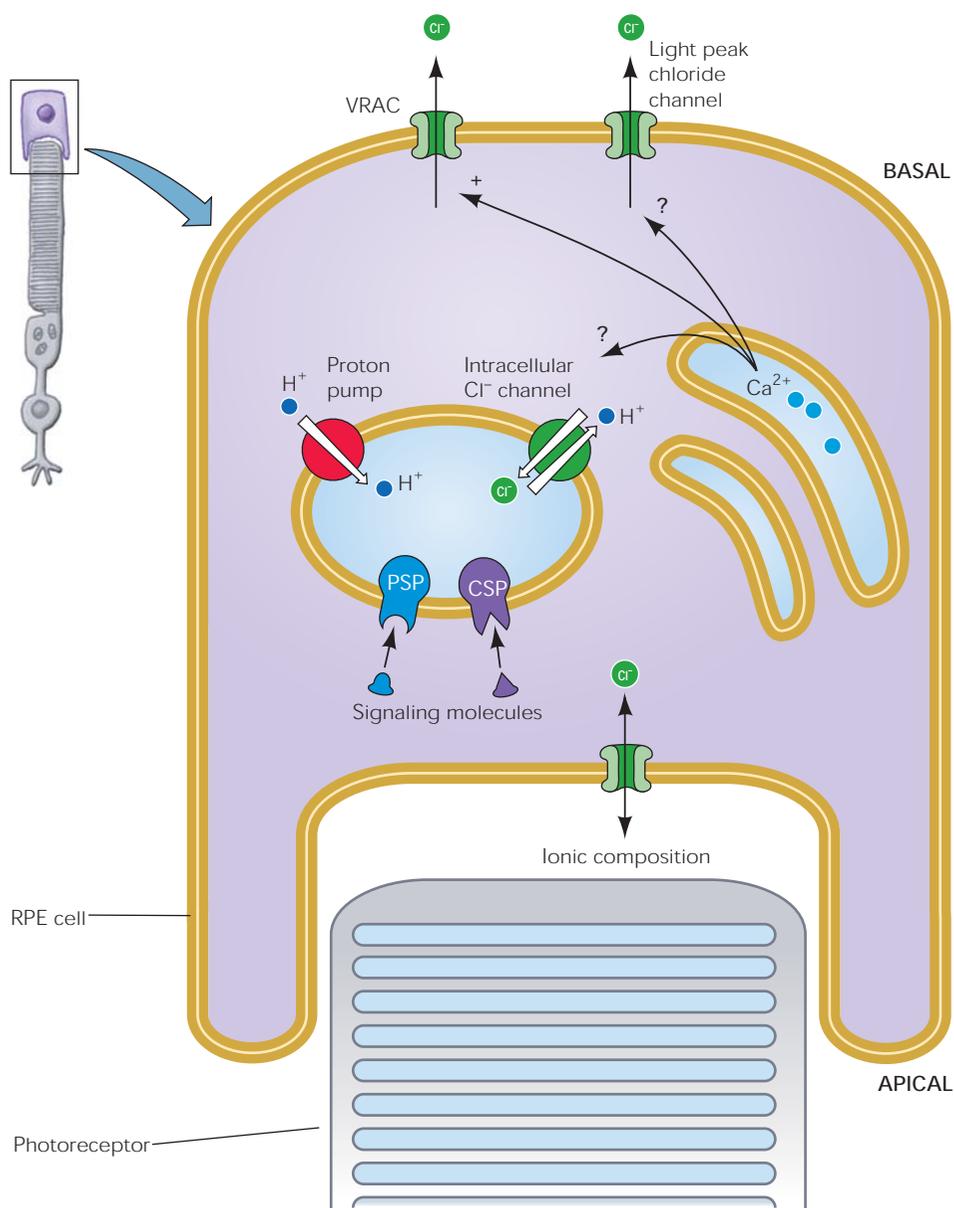
FIGURE 5. Functions of chloride channels in RPE
Depending on the conditions, retinal pigment epithelium (RPE) cells can function as an absorptive or secretory epithelium. The basolateral Cl⁻ channel responsible for the light peak regulates membrane potential and depolarizes the RPE in light. Intracellular Cl⁻ channels regulate vesicular pH and intraluminal Cl concentration, which affect both enzymes and receptors for cytoplasmic signaling molecules. CSP, Cl⁻-sensitive protein; PSP, pH-sensitive protein. Although there is no compelling evidence for Cl⁻ channels in the apical membrane, we hypothesize that Cl⁻ channels in the apical membrane may be involved in regulating the ionic composition of the solution bathing the photoreceptors under certain conditions. Volume-regulated anion channels (VRAC) regulate the cell volume. VRAC is presumably located in the basolateral membrane. Ca^{2+} may regulate the basolateral Cl⁻ channel, VRAC, and intracellular Cl⁻ channels as discussed in the text. The intracellular Cl⁻ channel is shown as a H^+/Cl^- exchanger because recent evidence has shown that certain intracellular ClC channels are transporters, as discussed in the text.

Cell volume regulation

The cell membrane cannot withstand more than 2 kPa osmotic pressure without bursting (28). Although 2 kPa corresponds to ~1 mM osmolyte concentration difference across the membrane, the cytoskeleton and extracellular matrix strengthen the membrane and allow considerably higher gradients to develop. A major mechanism that cells employ to avoid bursting is regulation of their volume in response to osmotic challenge. Cell swelling often activates K^+ and Cl⁻ channels that result in KCl and water efflux to return the cell to its original volume (regulatory volume decrease) (55). Conversely, cell shrinkage results in regulatory volume increase by mechanisms that involve decreases in ionic conductance.

It is not entirely clear what osmotic forces are experienced by RPE cells in the eye. The volume of the subretinal space increases at light onset as a consequence of K^+ and water movement out of the RPE (6, 34). Analysis of accumulation and depletion of ions in the subretinal space suggests, however, that the change in osmolarity may be small (16). Nevertheless, RPE cells express volume-regulated anion channels (9, 38) and the currents induced by bestrophins expressed in 293 cells are very sensitive to changes in cell volume (22). Another possible role for volume-sensitive Cl⁻ channels is in regulation of cell volume as a consequence of ingestion of photoreceptor discs as discussed below.

Intracellular Cl⁻ channels

Although it is clear that bestrophins can function as Cl⁻ channels at the plasma membrane, is it possible that they also have an intracellular function? Several of the ClC Cl⁻ channels, such as ClC-3 and ClC-7, have both plasma membrane and intracellular functions (35). One function of intracellular Cl⁻ channels is to regulate the pH of intracellular membrane compartments. For example, the luminal pH of the membrane compartments decreases along the endosomal pathway. The acidic luminal environment develops as a result of the vesicular proton pump that pumps protons against their concentration gradient into the organelle. To acidify the lumen, however, a counterion shunt pathway is required to dissipate the transmembrane potential that develops as protons accumulate in the lumen. This counterion shunt appears to be provided largely by Cl⁻ channels, at least in the endosomal pathway (20). The luminal pH of the vesicle is important in membrane trafficking

as well as in maintaining the function of the enzymes that reside within these organelles (20, 35, 50).

Immunostaining of 293 and HeLa cells overexpressing bestrophins reveal a large amount of bestrophin in intracellular compartments (62, 79). This is confirmed by cell-surface biotinylation (22, 61), which shows that a relatively small fraction of bestrophin is located on the cell surface. This subcellular distribution could be a consequence of overexpression, or it might reflect an intracellular role for bestrophin. Immunocytochemical localization of Best1 in retina has shown that Best1 is present near the basolateral plasma membrane of RPE cells, but the images also show that there is a significant fraction of Best1 that is in intracellular compartments (4, 46). Using both immunocytochemistry and subcellular fractionation (unpublished observations), we also found that in tissues that natively express bestrophins, a majority of the bestrophin appears to be intracellular. Although some of this could be bestrophin in the biosynthetic pathway, it raises the possibility that bestrophin might be playing a role in intracellular organelles.

RPE cells are extremely active phagocytes, so there is an exceptional amount of membrane traffic in these cells. As mentioned above, photoreceptors constantly renew their outer segments by shedding their most distal discs each morning. These discs are phagocytosed by the pigment epithelium and digested by a lysosomal pathway (5, 54). It has been estimated that each RPE cell may ingest >25,000 discs per day (54). Also, phagocytosis of photoreceptor discs by RPE involves the extension of specialized pseudopodia that is likely to involve vesicular membrane traffic (49, 78). Cl⁻ channels are likely to contribute not only to the maturation of the phagolysosome by controlling its pH and water content (1, 42) but also in regulating membrane traffic along the endosomal-lysosomal pathway. In liver cells, phagocytosis is accompanied by large osmolyte fluxes via

anion channels and transporters (87), and changes in extracellular osmolarity alter phagocytosis (82). The role of Cl⁻ channels in phagocytosis is underscored by the observation that phagocytosis is blocked by the Cl⁻ channel blocker tamoxifen (44).

Another emerging function of intracellular Cl⁻ channels is regulation of Ca^{2+} movement across the endoplasmic reticulum by providing a counterion pathway. Luminal Ca^{2+} concentration is important for protein folding and quality control in the endoplasmic reticulum (51), and Ca^{2+} imbalance in the endoplasmic reticulum can lead to cell death (80). Cl⁻ channels have been shown to be present in sarco(endo)plasmic reticulum, and Cl⁻ channel blockers alter Ca^{2+} uptake into the sarcoplasmic reticulum (59). One would speculate that if Ca^{2+}-activated Cl⁻ channels are present in the endoplasmic reticulum, increases in cytosolic Ca^{2+} would activate these and facilitate Ca^{2+} flux across the endoplasmic reticulum membrane.

Significance of calcium regulation

Overexpressed bestrophins have an EC_{50} for Ca^{2+} in the range of 200 nM (61, 62). If this represents the Ca^{2+} affinity of native channels, bestrophins would be expected to be at least partially activated at typical resting Ca^{2+} concentrations of 50–200 nM. At present, the physiological significance of the Ca^{2+} sensitivity of bestrophins is speculative. Although there are Ca^{2+}-stimulated Cl⁻ conductances in RPE (see references in Ref. 33), there is no direct evidence that the light peak of the dcERG is Ca^{2+} dependent. The role of Ca^{2+} in cell volume regulation is equivocal, although there is good evidence that Ca^{2+} may facilitate the regulatory volume decrease but is not obligatory (2). Finally, there is no information about how cytosolic Ca^{2+} might regulate Cl⁻ channels in intracellular vesicles.

Can Best Disease Provide Insights into the Mechanisms of AMD?

Although lipofuscinosis is thought to

be a causal factor in AMD, it is clear that the consequences of lipofuscin accumulation differ in Best disease and AMD (e.g., Refs. 25 and 56). AMD is typically characterized by deposits of debris called drusen between the RPE and Bruch's membrane (7, 25). Drusen contains proteins characteristic of immune processes, suggesting that it is produced as a consequence of inflammation (3, 13, 29, 30). This is interesting in light of the fact that specific polymorphisms in complement factor H correlate strongly with susceptibility to AMD (17, 30, 31). In contrast, in Best disease there are few or no drusen. If lipofuscin accumulation is causal to drusen formation in AMD, why is there only modest drusen formation in Best disease? Does it reflect complement factor H genotype, for example? The answer may also be hidden in our limited understanding of lipofuscin. The composition of lipofuscin appears to be different in AMD and Best disease (45), and its distribution is different. In AMD, the vitelliform egg-yolk-like lesions that are characteristic of Best disease are usually not present (56, 84). However, vitelliform lesions have been reported in individuals who have no known hBest1 mutations (65). Despite these differences between Best disease and AMD, elucidating the mechanisms of lipofuscin accumulation and toxicity will be an important step in understanding these diseases.

Dysfunction of Some ClC Cl⁻ Channels Produces Retinal Degeneration

There seems to be an interesting relationship between Cl⁻ channels, lipofuscinosis, and retinal degeneration. RPE cells express a variety of different kinds of Cl⁻ channels in addition to bestrophins. ClC-2, ClC-3, ClC-5, and CFTR have been identified by RT-PCR and Western blotting (86, 90). Electrophysiologi-cally, currents resembling ClC-2 and CFTR, as well as Ca^{2+}-activated and volume-activated Cl⁻ currents, have been described (24, 33). Interestingly, in mice that have had the ClC-2, ClC-3, or ClC-7

Cl⁻ channels knocked out, the retina degenerates (8, 39, 71). Retinal degeneration in the ClC-2 knockout may be due to an RPE dysfunction because RPE short-circuit current is reduced in ClC-2 knockout mice (8).

The mechanisms by which knockout of these genes produce retinal degeneration remain speculative. ClC-2 and ClC-3 are located both on the plasma membrane and in intracellular compartments. Their plasma membrane roles certainly include transepithelial transport. Dysfunction of these channels, therefore, would likely result in abnormal composition of fluid surrounding photoreceptors.

In addition to retinal degeneration, the ClC-3 and ClC-7 knockouts have a more generalized neurodegenerative disease resembling NCL (15, 27, 37, 52, 93). NCLs have been linked to mutations in eight genes (CLN1–CLN8). Several of these have been identified as lysosomal enzymes or components of lysosomes. ClC-7 is also localized in lysosomes (37). One hypothesis for the mechanism by which ClC-7 deletion produces an NCL-like disease and retinal degeneration is related to the role of Cl⁻ channels in regulating the pH of intracellular compartments (20). This hypothesis is attractive because changes in lysosomal pH have long been known to be associated with retinal degeneration. An increase in lysosomal pH can be produced by chloroquine, which is a weak base that accumulates in lysosomes. A common side effect of chloroquine therapy for autoimmune diseases is retinopathy associated with accumulation of lipofuscin (69, 75, 76).

Surprisingly, however, changes in lysosomal pH do not explain the NCL phenotype of the ClC-7 knockout, because lysosomal pH is normal in these animals (37). An alternative possibility that should be considered is that Cl⁻ concentration in the vesicle might itself be an important regulator of vesicular function, as we proposed previously (20). In yeast, for example, a ClC-like Cl⁻ channel is implicated in regulating the Cl⁻ concentration of Golgi compartments that is required for Cu²⁺ loading of an oxidase enzyme

(14). (See *Notes added in proof*, below).

Although the ClC-3 deletion was postulated to produce lipofuscinosis by reducing lysosomal enzyme activity or blocking maturation of lysosomes as a result of an elevated organellar pH (93), ClC-3 is not concentrated in lysosomes like ClC-7 but rather is found in endosomes and synaptic vesicles. This suggests that the phenotype of the ClC-3 knockout may be caused by another mechanism. Furthermore, another mouse strain with a similar ClC-3 deletion does not exhibit an NCL phenotype (37), implying that genetic background or other factors may be important.

Conclusions

The relationship between various chloride channels and lipofuscinosis suggests that neural degeneration in NCL and photoreceptor degeneration in macular degeneration may involve similar mechanisms. Our working hypothesis is that Cl⁻ channels may have multiple functions, both at the plasma membrane and in intracellular organelles. Defects in Cl⁻ channel function could result in retinal degeneration as a consequence of problems with cell volume regulation, function and trafficking of intracellular organelles, or regulation of the extracellular fluid surrounding outer segments. However, the fact that lipofuscin accumulation occurs in NCL as a consequence of lysosomal dysfunction suggests that the retinal degeneration that occurs in Best disease is also a lysosomal problem, especially because RPE cells are such active phagocytes. Understanding the mechanistic relationship between lipofuscin accumulation and chloride channels will provide valuable insights into the process of AMD (see below).

Notes added in proof

Recent data that certain intracellular ClCs are proton-Cl⁻ exchangers raises interesting questions about the role of ClCs in regulating vesicular pH. (58a, 66a).

An excellent review on the physiolo-

gy of RPE cells has recently been published. Interested readers should consult the review for more detail on this interesting cell type (73a). ∎

References

1. Al Awqati Q. Proton-translocating ATPases. *Annu Rev Cell Biol* 2: 179–199, 1986.

2. Altamirano J, Brodwick MS, and Alvarez-Leefmans FJ. Regulatory volume decrease and intracellular Ca²⁺ in murine neuroblastoma cells studied with fluorescent probes. *J Gen Physiol* 112: 145–160, 1998.

3. Anderson DH, Talaga KC, Rivest AJ, Barron E, Hageman GS, and Johnson LV. Characterization of beta amyloid assemblies in drusen: the deposits associated with aging and age-related macular degeneration. *Exp Eye Res* 78: 243–256, 2004.

4. Bakall B, Marmorstein LY, Hoppe G, Peachey NS, Wadelius C, and Marmorstein AD. Expression and localization of bestrophin during normal mouse development. *Invest Ophthalmol Vis Sci* 44: 3622–3628, 2003.

5. Besharse JC and Defoe D. The role of retinal pigment epithelium in photoreceptor membrane turnover. In: *The Retinal Pigment Epithelium*, edited by Marmor MF and Wolfensberger TJ. New York: Oxford University Press, 1998, p. 152–172.

6. Bialek S and Miller SS. K⁺ and Cl⁻ transport mechanisms in bovine pigment epithelium that can modulate subretinal space volume and composition. *J Physiol* 475: 401–417, 1994.

7. Bok D. New insights and new approaches toward the study of age-related macular degeneration. *Proc Natl Acad Sci USA* 99: 14619–14621, 2002.

8. Bosl MR, Stein V, Hubner C, Zdebik AA, Jordt SE, Mukhopadhyay AK, Davidoff MS, Holstein AF, and Jentsch TJ. Male germ cells and photoreceptors, both dependent on close cell-cell interactions, degenerate upon ClC-2 Cl⁻ channel disruption. *EMBO J* 20: 1289–1299, 2001.

9. Botchkin LM and Matthews G. Chloride current activated by swelling in retinal pigment epithelium cells. *Am J Physiol Cell Physiol* 265: C1037–C1045, 1993.

10. Caldwell GM, Kakuk LE, Griesinger IB, Simpson SA, Nowak NJ, Small KW, Maumenee IH, Rosenfeld PJ, Sieving PA, Shows TB, and Ayyagari R. Bestrophin gene mutations in patients with Best vitelliform macular dystrophy. *Genomics* 58: 98–101, 1999.

11. Clapham DE. The list of potential volume-sensitive chloride currents continues to swell (and shrink). *J Gen Physiol* 111: 623–624, 1998.

12. Cooper JD. Progress towards understanding the neurobiology of Batten disease or neuronal ceroid lipofuscinosis. *Curr Opin Neurol* 16: 121–128, 2003.

13. Crabb JW, Miyagi M, Gu X, Shadrach K, West KA, Sakaguchi H, Kamei M, Hasan A, Yan L, Rayborn ME, Salomon RG, and Hollyfield JG. Drusen proteome analysis: an approach to the etiology of age-related macular degeneration. *Proc Natl Acad Sci USA* 99: 14682–14687, 2002.

14. Davis-Kaplan SR, Askwith CC, Bengtzen AC, Radisky D, and Kaplan J. Chloride is an allosteric effector of copper assembly for the yeast multi-copper oxidase Fet3p: an unexpected role for intracellular chloride channels. *Proc Natl Acad Sci USA* 95: 13641–13645, 1998.

15. Dawson G and Cho S. Batten's disease: clues to neuronal protein catabolism in lysosomes. *J Neurosci Res* 60: 133–140, 2000.

16. Dmitriev AV, Govardovskii VI, Schwahn HN, and Steinberg RH. Light-induced changes of extracellular ions and volume in the isolated chick retina-pigment epithelium preparation. *Vis Neurosci* 16: 1157–1167, 1999.

17. Edwards AO, Ritter R III, Abel KJ, Manning A, Panhuysen C, and Farrer LA. Complement factor H polymorphism and age-related macular degeneration. *Science* 308: 421–424, 2005.

18. Eldred GE. Lipofuscin fluorophore inhibits lysosomal protein degradation and may cause early stages of macular degeneration. *Gerontology* 41: 15–28, 1995.

19. Eldred GE and Lasky MR. Retinal age pigments generated by self-assembling lysosomotropic detergents. *Nature* 361: 724–726, 1993.

20. Faundez V and Hartzell HC. Intracellular chloride channels: determinants of function in the endosomal pathway. *Science STKE* 2004: re8, 2004.

21. Finnemann SC, Leung LW, and Rodriguez-Boulan E. The lipofuscin component A2E selectively inhibits phagolysosomal degradation of photoreceptor phospholipid by the retinal pigment epithelium. *Proc Natl Acad Sci USA* 99: 3842–3847, 2002.

22. Fischmeister R and Hartzell C. Volume-sensitivity of the bestrophin family of chloride channels. *J Physiol* 562: 477–491, 2004.

23. Fujii S, Gallemore RP, Hughes BA, and Steinberg RH. Direct evidence for a basolateral membrane Cl⁻ conductance in toad retinal pigment epithelium. *Am J Physiol Cell Physiol* 262: C374–C383, 1992.

24. Gallemore RP, Hughes BA, and Miller SS. Retinal pigment epithelial transport mechanisms and their contributions to the electroretinogram. *Prog Retinal Eye Res* 16: 509–566, 1997.

25. Gass JDM. *Stereoscopic Atlas of Macular Diseases: Diagnosis and Treatment.* St. Louis, MO: C. V. Mosby, 1987.

26. Gibson A, Lewis AP, Affleck K, Meldrum E, and Thompson N. hCLCA1 and mCLCA3 are secreted non-integral membrane proteins and therefore are not ion channels. *J Biol Chem* 280: 27205–27212, 2005.

27. Goebel HH and Wisniewski KE. Current state of clinical and morphological features in human NCL. *Brain Pathol* 14: 61–69, 2004.

28. Guharay F and Sachs F. Stretch-activated single ion channel currents in tissue-cultured embryonic chick skeletal muscle. *J Physiol* 352: 685–701, 1984.

29. Hageman GS, Luthert PJ, Victor Chong NH, Johnson LV, Anderson DH, and Mullins RF. An integrated hypothesis that considers drusen as biomarkers of immune-mediated processes at the RPE-Bruch's membrane interface in aging and age-related macular degeneration. *Prog Retinal Eye Res* 20: 705–732, 2001.

30. Hageman GS, Anderson DH, Johnson LV, Hancox LS, Taiber AJ, Hardisty LI, Hageman JL, Stockman HA, Borchardt JD, Gehrs KM, Smith RJH, Silvestri G, Russell SR, Klaver CCW, Barbazetto I, Chang S, Yannuzzi LA, Barile GR, Merriam JC, Smith RT, Olsh AK, Bergeron J, Zernant J, Merriam JE, Gold B, Dean M, and Allikmets R. A common haplotype in the complement regulatory gene factor H (HF1/CFH) predisposes individuals to age-related macular degeneration. *Proc Natl Acad Sci USA* 102: 7227–7232, 2005.

31. Haines JL, Hauser MA, Schmidt S, Scott WK, Olson LM, Gallins P, Spencer KL, Kwan SY, Noureddine M, Gilbert JR, Schnetz-Boutaud N, Agarwal A, Postel EA, and Pericak-Vance MA. Complement factor H variant increases the risk of age-related macular degeneration. *Science* 308: 419–421, 2005.

32. Hartzell HC, Putzier I, and Arreola J. Calcium-activated chloride channels. *Annu Rev Physiol* 67: 715–758, 2005.

33. Hartzell HC and Qu Z. Chloride currents in acutely isolated *Xenopus* retinal pigment epithelial cells. *J Physiol* 549: 453–469, 2003.

34. Huang B and Karwoski CJ. Light-evoked expansion of subretinal space volume in the retina of the frog. *J Neurosci* 12: 4243–4252, 1992.

35. Jentsch TJ, Stein V, Weinreich F, and Zdebik AA. Molecular structure and physiological function of chloride channels. *Physiol Rev* 82: 503–568, 2002.

36. Karlin A and Akabas MH. Substituted-cysteine accessibility method. *Methods Enzymol* 293: 123–145, 1998.

37. Kaspar D, Planells-Cases R, Fuhrmann JC, Scheel O, Zeitz O, Ruether K, Poet M, Steinfeld R, Schweizer M, Kornak U, and Jentsch JT. Loss of the chloride channel ClC-7 leads to lysosomal storage disease and neurodegeneration. *EMBO J* 24: 1079–1091, 2005.

38. Kennedy BG. Volume regulation in cultured cells derived from human retinal pigment epithelium. *Am J Physiol Cell Physiol* 266: C676–C683, 1994.

39. Kornak U, Kasper D, Bosl MR, Kaiser E, Schweizer M, Schulz A, Friedrich W, Delling G, and Jentsch TJ. Loss of the ClC-7 chloride channel leads to the osteoporosis in mice and men. *Cell* 104: 205–215, 2001.

40. Kramer F, Stohr H, and Weber BH. Cloning and characterization of the murine Vmd2 RFP-TM gene family. *Cytogenetics Genome Res* 105: 107–114, 2004.

41. Linsenmeier RA and Steinberg RH. Origin and sensitivity of the light peak in the intact cat eye. *J Physiol* 331: 653–673, 1982.

42. Lukacs GL, Rotstein OD, and Grinstein S. Determinants of the phagosomal pH in macrophages. In situ assessment of vacuolar H⁺-ATPase activity, counterion conductance, and H⁺ "leak." *J Biol Chem* 266: 24540–24548, 1991.

43. Ma D, Zerangue N, Raab-Graham K, Fried SR, Jan YN, and Jan LY. Diverse trafficking patterns due to multiple traffic motifs in G protein-activated inwardly rectifying potassium channels from brain and heart. *Neuron* 33: 715–729, 2002.

44. Mannerstrom M, Maenpaa H, Toimela T, Salminen L, and Tahti H. The phagocytosis of rod outer segments is inhibited by selected drugs in retinal pigment epithelial cell cultures. *Pharmacol Toxicol* 88: 27–33, 2001.

45. Marmorstein AD, Marmorstein LY, Sakaguchi H, and Hollyfield JG. Spectral profiling of autofluorescence associated with lipofuscin, Bruch's membrane, and sub-RPE deposits in normal and AMD eyes. *Invest Ophthalmol Vis Sci* 43: 2435–2441, 2002.

46. Marmorstein AD, Mormorstein LY, Rayborn M, Wang X, Hollyfield JG, and Petrukhin K. Bestrophin, the product of the Best vitelliform macular dystrophy gene (VMD2), localizes to the basolateral membrane of the retinal pigment epithelium. *Proc Natl Acad Sci USA* 97: 12758–12763, 2000.

47. Marmorstein AD, Stanton JB, Yocom J, Bakall B, Schiavone MT, Wadelius C, Marmorstein LY, and Peachey NS. A model of best vitelliform macular dystrophy in rats. *Invest Ophthalmol Vis Sci* 45: 3733–3739, 2004.

48. Marquardt A, Stohr H, Passmore LA, Kramer F, Rivera A, and Weber BH. Mutations in a novel gene, VMD2, encoding a protein of unknown properties cause juvenile-onset vitelliform macular dystrophy (Best's disease). *Hum Mol Genet* 7: 1517–1525, 1998.

49. Matsumoto B, Defoe DM, and Besharse JC. Membrane turnover in rod photoreceptors: ensheathment and phagocytosis of outer segment distal tips by pseudopodia of the retinal pigment epithelium. *Proc R Soc Lond B Biol Sci* 230: 339–354, 1987.

50. Mellman I. The importance of being acid: the role of acidification in intracellular membrane traffic. *J Exp Biol* 172: 39–45, 1992.

51. Michalak M, Robert Parker JM, and Opas M. Ca²⁺ signaling and calcium binding chaperones of the endoplasmic reticulum. *Cell Calcium* 32: 269–278, 2002.

52. Mitchison HM, Lim MJ, and Cooper JD. Selectivity and types of cell death in the neuronal ceroid lipofuscinoses. *Brain Pathol* 14: 86–96, 2004.

53. Musarella MA. Molecular genetics of macular degeneration. *Doc Ophthalmol* 102: 165–177, 2001.

54. Nguyen-Legros J and Hicks D. Renewal of photoreceptor outer segments and their phagocytosis by the retinal pigment epithelium. *Int Rev Cytol* 196: 245–313, 2000.

55. Nilius B, Eggermont J, Voets T, Buyse G, Manolopoulos V, and Droogmans G. Properties of volume-regulated anion channels in mammalian cells. *Prog Biophys Mol Biol* 68: 69–119, 1997.

56. O'Gorman S, Flaherty WA, Fishman GA, and Berson EL. Histopathologic findings in Best's vitelliform macular dystrophy. *Arch Ophthalmol* 106: 1261–1268, 1988.

57. Penfold PL, Madigan MC, Gillies MC, and Provis JM. Immunological and aetiological aspects of macular degeneration. *Prog Retinal Eye Res* 20: 385–414, 2001.

58. Petrukhin K, Koisti MJ, Bakall B, Li W, Xie G, Marknell T, Sandgren O, Forsman K, Holmgren G, Andreasson S, Vujic M, Bergen AAB, McGarty-Dugan V, Figueroa D, Austin CP, Metzker ML, Caskey CT, and Wadelius C. Identification of the gene responsible for Best macular dystrophy. *Nat Genet* 19: 241–247, 1998.

58a. Picollo A and Pusch M. Chloride/proton antiporter activity of mammalian ClC proteins ClC-4 and ClC-5. *Nature* 436: 420–423, 2005.

59. Pollock NS, Kargacin ME, and Kargacin GJ. Chloride channel blockers inhibit Ca²⁺ uptake by the smooth muscle sarcoplasmic reticulum. *Biophys J* 75: 1759–1766, 1998.

60. Pusch M. Ca²⁺-activated chloride channels go molecular. *J Gen Physiol* 123: 323–325, 2004.

61. Qu Z, Fischmeister R, and Hartzell HC. Mouse bestrophin-2 is a bona fide Cl⁻ channel: identification of a residue important in anion binding and conduction. *J Gen Physiol* 123: 327–340, 2004.

62. Qu Z, Wei RW, Mann W, and Hartzell HC. Two bestrophins cloned from *Xenopus laevis* oocytes express Ca-activated Cl currents. *J Biol Chem* 278: 49563–49572, 2003.

63. Qu Z and Hartzell HC. Determinants of anion permeation in the second transmembrane domain of the mouse bestrophin-2 chloride channel. *J Gen Physiol* 124: 371–382, 2004.

64. Quinn RH, Quong JN, and Miller SS. Adrenergic receptor activated ion transport in human fetal retinal pigment epithelium. *Invest Ophthalmol Vis Sci* 42: 255–264, 2001.

65. Renner AB, Tillack H, Kraus H, Kramer F, Mohr N, Weber BH, Foerster MH, and Kellner U. Late onset is common in best macular dystrophy associated with VMD2 gene mutations. *Ophthalmology* 112: 586–592, 2005.

66. Rymer J, Miller SS, and Edelman JL. Epinephrine-induced increases in $[Ca^{2+}]_{in}$ and KCl-coupled fluid absorption in bovine RPE. *Invest Ophthalmol Vis Sci* 42: 1921–1929, 2001.

66a. Scheel O, Zdebik A, Lourdel S, and Jentsch TJ. Voltage-dependent electrogenic chloride/proteon excahnge by endosomal ClC proteins. *Nature* 436: 424–427, 2005.

67. Schutt F, Ueberle B, Schnolzer M, Holz FG, and Kopitz J. Proteome analysis of lipofuscin in human retinal pigment epithelial cells. *FEBS Lett* 528: 217–221, 2002.

68. Shamsi FA and Boulton M. Inhibition of RPE lysosomal and antioxidant activity by the age pigment lipofuscin. *Invest Ophthalmol Vis Sci* 42: 3041–3046, 2001.

69. Shroyer NF, Lewis RA, and Lupski JR. Analysis of the ABCR (ABCA4) gene in 4-aminoquinoline retinopathy: is retinal toxicity by chloroquine and hydroxychloroquine related to Stargardt disease? *Am J Ophthalmol* 131: 761–766, 2001.

70. Sparrow JR and Cai B. Blue light-induced apoptosis of A2E-containing RPE: involvement of caspase-3 and protection by Bcl-2. *Invest Ophthalmol Vis Sci* 42: 1356–1362, 2001.

71. Stobrawa SM, Breiderhoff T, Takamori S, Engel D, Schweizer M, Zdebik AA, Bosl MR, Ruether K, Jahn H, Draguhn A, Jahn R, and Jentsch TJ. Disruption of ClC-3, a chloride channel expressed on synaptic vesicles, leads to a loss of the hippocampus. *Neuron* 29: 185–196, 2001.

72. Stohr H, Marquardt A, Nanda I, Schmid M, and Weber BH. Three novel human VMD2-like genes are members of the evolutionary highly conserved RFP-TM family. *Eur J Hum Genet* 10: 281–284, 2002.

73. Stone EM, Sheffield VC, and Hageman GS. Molecular genetics of age-related macular degeneration. *Hum Mol Genet* 10: 2285–2292, 2001.

73a. Strauss O. The retinal pigment epithelium in visual function. *Physiol Rev* 85: 845–881, 2005.

74. Sun H, Tsunenari T, Yau KW, and Nathans J. The vitelliform macular dystrophy protein defines a new family of chloride channels. *Proc Natl Acad Sci USA* 99: 4008–4013, 2002.

75. Sundelin SP and Terman A. Different effects of chloroquine and hydroxychloroquine on lysosomal function in cultured retinal pigment epithelial cells. *APMIS* 110: 481–489, 2002.

76. Toimela T, Salminen L, and Tahti H. Effects of tamoxifen, toremifene and chloroquine on the lysosomal enzymes in cultured retinal pigment epithelial cells. *Pharmacol Toxicol* 83: 246–251, 1998.

77. Tsuboi S and Pederson JE. Volume transport across the isolated retinal pigment epithelium of cynomolgus monkey eyes. *Invest Ophthalmol Vis Sci* 29: 1652–1655, 1988.

78. Tsukamoto Y. Pigment epithelial ensheathment and phagocytosis of rod tips in the retina of *Rana catesbeiana*. *J Morphol* 188: 303–313, 1986.

79. Tsunenari T, Sun H, Williams J, Cahill H, Smallwood P, Yau KW, and Nathans J. Structure-function analysis of the bestrophin family of anion channels. *J Biol Chem* 278: 41114–41125, 2003.

80. Verkhratsky A and Toescu EC. Endoplasmic reticulum Ca^{2+} homeostasis and neuronal death. *J Cell Mol Med* 7: 351–361, 2003.

81. Wajima R, Chater SB, Katsumi O, Mehta MC, and Hirose T. Correlating visual acuity and electrooculogram recordings in Best's Disease. *Ophthalmologe* 207: 174–181, 1993.

82. Warskulat U, Zhang F, and Haussinger D. Modulation of phagocytosis by anisoosmolarity and betaine in rat liver macrophages (Kupffer cells) and RAW 264.7 mouse macrophages. *FEBS Lett* 391: 287–292, 1996.

84. Weingeist TA, Kobrin JL, and Watzke RC. Histopathology of Best's macular dystrophy. *Arch Ophthalmol* 100: 1108–1114, 1982.

85. Weleber RG. Fast and slow oscillations of the electro-oculogram in Best's macular dystrophy and retinitis pigmentosa. *Arch Ophthalmol* 107: 530–537, 1989.

86. Weng TX, Godley BF, Jin GF, Mangini NJ, Kennedy BG, Yu ASL, and Wills NK. Oxidant and antioxidant modulation of chloride channels expressed in human retinal pigment epithelium. *Am J Physiol Cell Physiol* 283: C839–C849, 2002.

87. Wettstein M, Peters-Regehr T, Kubitz R, Fischer R, Holneicher C, Monnighoff I, and Haussinger D. Release of osmolytes induced by phagocytosis and hormones in rat liver. *Am J Physiol Gastrointest Liver Physiol* 278: G227–G233, 2000.

88. White K, Marquardt A, and Weber BHF. VMD2 mutations in vitelliform macular dystrophy (Best disease) and other maculopathies. *Hum Mutat* 15: 301–308, 2000.

89. White SH and Wimley WC. Membrane protein folding and stability: physical principles. *Annu Rev Biophys Biomol Struct* 28: 319–365, 1999.

90. Wills NK, Weng T, Mo L, Hellmich HL, Yu A, Wang T, Buchheit S, and Godley BF. Chloride channel expression in cultured human fetal RPE cells: response to oxidative stress. *Invest Ophthalmol Vis Sci* 41: 4247–4255, 2000.

91. Wu J, Peachey NS, and Marmorstein AD. Light-evoked responses of the mouse retinal pigment epithelium. *J Neurophysiol* 91: 1134–1142, 2004.

92. Yardley J, Leroy BP, Hart-Holden N, Lafaut BA, Loeys B, Messiaen LM, Perveen R, Reddy MA, Bhattacharya SS, Traboulsi E, Baralle D, De Laey JJ, Puech B, Kestelyn P, Moore AT, Manson FD, and Black GC. Mutations of VMD2 splicing regulators cause nanophthalmos and autosomal dominant vitreoretinochoroidopathy (ADVIRC). *Invest Ophthalmol Vis Sci* 45: 3683–3689, 2004.

93. Yoshikawa M, Uchida S, Ezaki J, Rai T, Hayama A, Kobayashi K, Kida Y, Noda M, Koike M, Uchiyama Y, Marumo F, Kominami E, and Sasaki S. CLC-3 deficiency leads to phenotypes similar to human neuronal ceroid lipofuscinosis. *Genes Cells* 7: 597–605, 2002.

94. Young RW. Pathophysiology of age-related macular degeneration. *Surv Ophthalmol* 31: 291–306, 1987.